JOURNAL OF GEOPHYSICAL RESEARCH, VOL. 91, NO. A12, PAGES 13,473-13,482, DECEMBER 1, 1986

MODEL PREDICTIONS OF SUBIONOSPHERIC VLF SIGNAL PERTURBATIONS RESULTING FROM LOCALIZED, ELECTRON PRECIPITATION-INDUCED IONIZATION ENHANCEMENT REGIONS

A. Tolstoy[1] and T. J. Rosenberg

Institute for Physical Science and Technology, University of Maryland, College Park

U. S. Inan and D. L. Carpenter

Space, Telecommunications and Radioscience Laboratory, Stanford University, Stanford, California

Abstract. Whistler-induced precipitation of energetic electrons produces transient ionospheric conductivity variations that perturb the amplitude and phase of VLF signals propagating in the earth-ionosphere waveguide (i.e., Trimpi events). This study uses a waveguide mode theoretic propagation model to predict the effect of localized ionization enhancement (IE) regions on nighttime long-path VLF signals from the U.S. Navy navigational transmitters NSS, NAA, NLK and NPM to Antarctic receiving stations, principally the U.S. station at Palmer. These predictions are then compared with the observed signal behavior in Trimpi events from which inferences can be drawn about an IE region's approximate location, size, and particle characteristics. The propagation model considers multiple modes, variable ground conductivity, and mode conversion. IE regions of variable length (typically 50-150 km) and distance from the receiver (up to 600 km) were considered. The conductivity change within an IE region was modeled by exponential electron density profiles modified by precipitated monoenergetic fluxes of 50- to 150-keV electrons. Our calculations show that some signal paths are more sensitive than others to perturbation by IE regions and that the size of an IE region is less important than its distance from the receiver. For a specified flux, higher-energy electrons produce larger effects than lower energy electrons; for a specified energy, larger fluxes will produce larger signal changes. For the particular case of 150-keV electrons precipitating into an ionosphere with VLF reflection height of 87 km, the received signal was largely insensitive to increasing the electron flux above $\sim 10^{-5}$ erg cm^{-2} s^{-1}. This flux is equivalent to $\sim 3 \times 10^{-3}$ erg cm^{-2} s^{-1} for E > 40 keV and an exponential energy spectrum with e-folding energy in the range 40 - 100 keV. The measured electron fluxes precipitated by lightning are of the same order. Higher saturation flux levels would apply in situations where the normal VLF reflection height was lower over that portion of a path where the whistler-induced precipitation was occurring. This study also examines the effects of transmitter-induced electron precipitation on the VLF signals. Such precipitation is known to occur and, as shown here, may on occasion have important effects on certain signals.

[1]Now at: Naval Research Laboratory, Washington, D. C.

Paper number 6A8483.
0148-0227/86/006A-8483$05.00

1. Introduction

One of the techniques that is being developed to study the burst precipitation of energetic electrons from the magnetosphere considers the perturbations to subionospherically propagating VLF signals that are caused by transient ionospheric electron density variations [Carpenter et al., 1985]. Impulsive disturbances affecting the amplitude of NSS and NAA transmissions received at Eights and Byrd stations in the Antarctic were first reported by Helliwell et al. [1973] who showed that they were correlated with the occurrence of whistlers. Later, Dingle and Carpenter [1981] showed that similar amplitude perturbations were also associated with other kinds of transient radio wave emissions. The first examples of rapid phase changes correlated with whistlers were reported by Lohrey and Kaiser [1979] on the low-latitude path from NWC, West Australia, to Dunedin, New Zealand. Subsequent measurements have shown that amplitude and phase are affected by whistler-induced perturbations on a wide variety of VLF signal paths [Carpenter and LaBelle, 1982; Leyser et al., 1984; Kintner and LaBelle, 1984; Carpenter et al., 1985; Inan et al., 1985] and at frequencies in the LF and MF range as well [Carpenter et al., 1984].

Such perturbations occur for nighttime signal paths which are believed to pass under or near the magnetospheric propagation paths over which the whistler or noise burst is propagating. These events, often referred to as "Trimpi" events after the observer who first noted them, are characterized by steep amplitude increases (or decreases) of up to 6 dB over a time interval of 0.5 - 2 seconds, followed by a slower return (~ 30 s) to preevent levels. The recovery is attributed to ionospheric response time and is consistent with estimates of effective recombination rates and electron densities in the height range of interest [Dingle, 1977].

These particular types of signal changes are hypothesized to result from localized ionization enhancement (IE) regions produced by electrons precipitating into the D region. Cyclotron resonance pitch angle scattering of radiation belt trapped electrons by the whistlers or noise emissions was suggested to be the precipitation mechanism [Helliwell et al., 1973; Dingle and Carpenter, 1981]. This followed from earlier direct evidence of electron and X ray burst precipitation associated with whistler-triggered and other discrete VLF emissions [Rosenberg et al., 1971, 1981; Rycroft, 1973; Foster and Rosenberg, 1976; Helliwell et al., 1980; see also Doolittle and Carpenter, 1983] and has been further confirmed by the recent satellite and rocket-based

TABLE 1. VLF Transmitting and Receiving Stations

	Frequency, kHz	Radiated Power, kW	Geographic Latitude, deg	Geographic Longitude, deg	L Value	Great Circle Distance, Mm to Eights	to Palmer	to Siple
Transmitter								
NAA (Cutler, Maine)	17.8	1000	44.6N	67.3W	3.21	13.3	12.2	13.45
NLK (Jim Creek, Washington)	18.6	850	48.2N	121.9W	3.02	14.1	13.5	14.1
NPM (Lua Luaiei, Hawaii)	23.4	300	21.4N	158.15W	1.12	12.0	12.3	11.9
NSS* (Annapolis, Maryland)	21.4 (new) 22.3 (old)	265	39.0N	76.45W	2.74	12.7	11.6	12.8
Receiver								
Eights			75S	77W	4.1			
Palmer			65S	64W	2.3			
Siple			76S	84W	4.1			

*For Eights measurements the NSS frequency was 22.3 kHz. For Palmer and Siple measurements the NSS frequency was 21.4 kHz.

measurements of Voss et al. [1984] and Goldberg et al. [1986]. These latter studies measured lightning-induced precipitation rates of the order of 10^{-3} erg cm^{-2} s^{-1} for electrons $\geq$ 50 keV, rates which are consistent with those derived by Chang and Inan [1985].

The localized ionization enhancements resulting from electron precipitation perturb the normal nighttime ionospheric VLF reflecting height at 85-87 km [Ferguson, 1980] and consequently alter the propagation characteristics of the earth-ionosphere waveguide. This, plus the fact that Trimpi events have not been observed under daytime conditions in the region of ionospheric perturbation when the normal reflecting height is 70-72 km and whistler activity is high, indicates that the major particle energies involved in the process are in the range 40-200 keV. Electrons with energies extending to ~ 300 keV are appropriate for cyclotron resonance with whistler frequencies within and near the plasmasphere [Chang and Inan, 1983, 1985].

In this paper we shall examine in detail the possible locations and characteristics of IE regions which can produce Trimpi events, as may be deduced by model predictions of propagation behavior changes resulting from the various ionospheric modifications. The scope of this paper is limited mainly to a consideration of amplitude effects for several of the long signal paths to Antarctica on which the effects have been commonly observed. However, the approach described here gives phase information as well, and some of these results are also presented. Details of the VLF transmitting and receiving stations, and the path geometries, are provided in Table 1 and Figure 1.

The two-dimensional Budden-Wait-Pappert [Budden, 1961; Wait, 1970; Pappert and Snyder, 1972] propagation model allowing for range and height variability but not for cross-range variability (transverse to great circle path) has been used. This model incorporates as much realism as is currently possible, including mode conversion and variable ground conductivity (see also Tolstoy [1983]). In subionospheric VLF propagation, radio waves are confined to the space between the earth and the ionosphere where the energy can be considered to be partitioned among a series of complex modes. Each mode represents a resonance condition for the waveguide, and the number of such modes needed to adequately represent the field is proportional to the waveguide height measured in source wavelengths; e.g., on the order of 12 modes are required at 20 kHz under nighttime conditions. For a given source-receiver path or path segment the complete set of modes is determined by a computer program called MODESRCH [Morfitt and Shellman, 1976]. However, at ranges beyond several thousand kilometers from the source only the lowest order modes, i.e., those most strongly

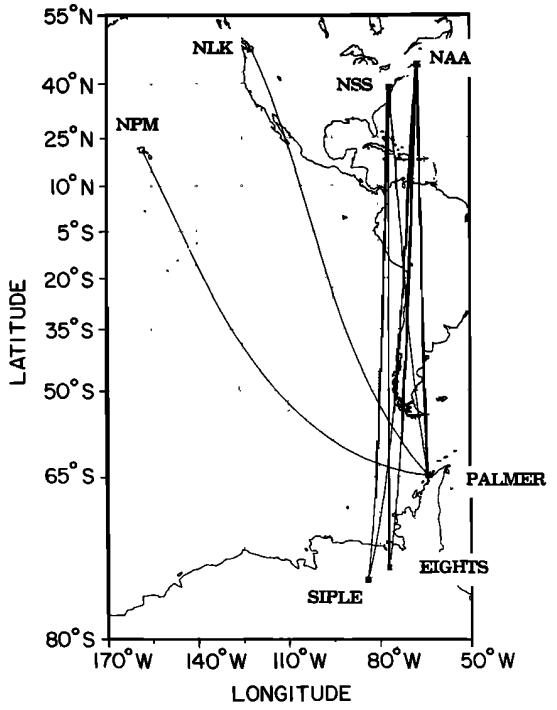

Fig. 1. Great circle paths from VLF transmitters NAA, NLK, NPM and NSS to Antarctic receiving stations Eights, Palmer and Siple.

TABLE 2. Background Nighttime Ionospheric Parameters (h',β) for Exponential Electron Density Distributions [Ferguson, 1980]

Season	h', km	β, per km	Magnetic Dip, degrees
Summer	87	0.0077f + 0.31 (0.45 for f=17.8, 0.45 for f=18.6, 0.47 for f=21.4, 0.48 for f=22.3, 0.49 for f=23.4)	all
Winter	87	0.0077f + 0.310	≤ 70
	85.6	0.0132f + 0.243	71
	84.2	0.0187f + 0.176	72
	82.8	0.0241f + 0.109	73
	81.4	0.0296f + 0.042	74
	80	0.0350f - 0.025	≥ 75

Here f is transmitter frequency in kilohertz (10 to 35).

excited and having smallest attenuation rates, contribute significant energy to the field. Consequently, for long paths encountering no abrupt changes in environmental parameters we retained only the five strongest modes for consideration. Otherwise, for short paths or for path segments in regions of abrupt changes such as ground conductivity changes from seawater to ice or transitions into or from IE regions, we retained the complete mode set represented by 15 modes.

Within the IE regions considered the modified electron density profiles were obtained by adding the ionization effects of specified incident electron energies and flux levels to the standard exponential background profile. A scheme to extend the two-dimensional model to quasi-three-dimensional so as to account for the more realistic geometry of the localized IE regions has been described [Tolstoy and Rosenberg, 1985], but not yet implemented.

2. Background Ionospheric Conditions

The ionosphere consists of a number of ionized regions above the earth's surface, each of which affects a different regime of radio wave frequencies. At VLF frequencies (3-30 kHz), the portion of the ionospheric D region from 60 to 90 km above the earth's surface most strongly influences subionospheric waveguide propagation. In this height range, and under quiet conditions, it can be shown that ions will give no observable effects [Budden, 1961; Thomas, 1969]. Consequently, at the heights of interest here a description of the ionospheric medium must include consideration of the earth's magnetic field and of the electron density (N) and electron-neutral collision frequency (ν) distributions. The modeling of the geomagnetic field is straightforward and is based upon a multipole expansion in terms of spherical harmonics [see Cain et al., 1967]. However, the modeling of N and ν is not as well understood and so is somewhat more controversial.

Considerable theoretical work in VLF propagation has been done over the last 20 years. As a result it is known that small changes in ionospheric parameters, e.g., changes of 5 km in the effective reflection height of a nighttime ionosphere, can result in up to 20-dB changes in signal amplitude calculations [Ferguson, 1980]. Consequently, accuracy in the description of the ionospheric medium is crucial.

The background nighttime exponential profiles for electron density and collision frequency in general use for VLF modeling [Wait and Spies, 1964] are given by

$$N(z) = 1.427 \times 10^{7} \exp(-\beta h' + (\beta - 0.15)z) \quad (1)$$

$$\nu(z) = 1.816 \times 10^{11} \exp(-0.15z) \quad (2)$$

where h' is reference height (kilometers), β is electron density gradient (per kilometer), and z is height above the surface of the earth (kilometers).

According to Ferguson [1980] the values of the reference height and electron density gradient given in Table 2 provide the most accurate description of the nighttime background electron density in the lower ionosphere. Note the variation of the parameter β with frequency. This indicates that N(z) must be approximated by slightly different exponentials at the different height levels interacting with each signal frequency. It is also interesting to note the winter enhancement of electron density for large magnetic dip.

3. Modification of Background Conditions

3.1. Whistler-Induced Changes

The main hypothesis behind this study is that an observed VLF signal perturbation occurring nearly simultaneously with the reception of a whistler is the result of that particular whistler inducing electron precipitation down to heights sufficient to alter the upper VLF waveguide boundary in a limited region and consequently affect the wave propagation. Direct evidence linking measurements of whistler-induced electron precipitation to VLF signal perturbations has only recently been obtained [Voss et al., 1984]. Although estimates have been made of lightning-induced electron precipitation [Chang and Inan, 1985], quantitative relationships showing how the magnitude of the signal perturbation depends on size and location of the perturbed region and on the particle flux and spectra have only been attempted on a first-order basis [Inan et al., 1985].

Since experimental data on the flux and spectra of electrons precipitated by whistlers are usually not available, we used the computer program TANGLE (courtesy of R. Vondrak and based on the work of Rees [1963]) to calculate the change in electron density profile produced by specified incident electron energies and fluxes. The modified profiles (see Figure 2) used to represent conditions in IE regions were calculated for monoenergetic spectra covering a range of electron energies (50-150 keV) and fluxes (10^{-7} to 10^{-3} erg cm^{-2} s^{-1}) considered to be representative of the Trimpi effect. The effects of very localized regions (10 - 150 km in length) were examined with these modified profiles.

From case studies of Trimpi events observed on paths from NSS and NLK to Palmer station, Carpenter and LaBelle [1982] concluded that the IE regions are located within 500 km of Palmer and

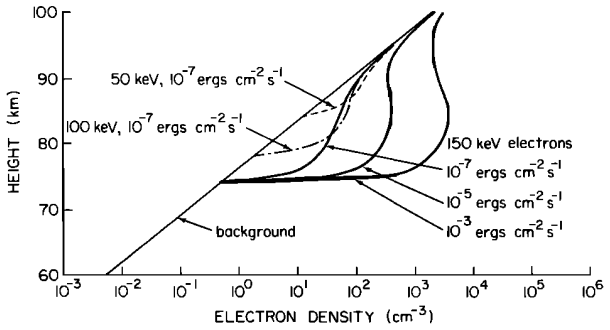

Fig. 2. Examples of modified electron density profiles for ionization enhancement (IE) regions resulting from the indicated energies and fluxes of precipitated electrons. The nighttime background exponential profile is characterized by h' = 87 km, $\beta = 0.47$ km^{-1}.

that an individual region, associated with a particular whistler path, could be less than 200 km in east-west extent. Subsequent measurements that included NPM at Palmer and represented a larger number of observing days have supported these initial findings, but also show that perturbed regions can occur as far as 1800 km from the receiving station [Leyser et al., 1984]. Moreover, multiple precipitation regions can exist, distributed in latitude and longitude over distances of the order of 500 km [Carpenter et al., 1984].

3.2. Transmitter-Induced Changes

Electron measurements on low-altitude satellites and rockets have provided evidence of electron precipitation induced by ground-based VLF transmitters [Imhof et al., 1981, 1983; Goldberg et al., 1983]. Such precipitation has so far been detected in relatively few cases. In addition, recent observations of whistler-induced perturbations on subionospheric VLF signals originating at very low southern latitudes [Inan et al., 1985] (where overhead precipitation would not be expected) indicate that precipitation regions near the source may only be involved in selected cases. Nevertheless it is worthwhile to investigate the possible significance of this effect.

Estimates have been made of the size and intensity of electron precipitation zones that may exist around VLF transmitters under appropriate nighttime ducting conditions [Inan, 1981; Inan et al., 1984]. As an example, Figure 3 illustrates the latitudinal profiles of precipitated electron flux and energy in the vicinity of NSS predicted to arise from wave-particle scattering interactions of the transmitter signal with trapped radiation. We have analyzed the effect of such zones on VLF propagation by using program TANGLE to convert the estimates of electron energy distributions and fluxes to equivalent modified electron density profiles and by subsequently incorporating those profiles into the propagation model.

4. Model Calculations

In general, nighttime paths longer than six or seven thousand kilometers are usually characterized by one strongly dominant mode. When a single mode encounters a region of increased electron density, its attenuation is increased and its phase is advanced. If only one mode is needed to describe the signal near an IE region (and mode conversion is not considered), then the signal amplitude would be expected to decrease (as a consequence of both spreading and absorption losses) and the phase to advance after encountering the region. However, if two or more modes are required to represent the signal, then amplitude increases and phase retardations may result as the mode interference pattern is changed.

The NSS to Eights station path for which frequent, large increases (up to 6 dB) had been reported [Helliwell et al., 1973] was examined in an earlier study [Tolstoy et al., 1982] using a propagation model which included neither mode conversion nor the very low conductivity effects of Antarctic ice. Those results showed that a single IE region located anywhere on the great circle path could not reproduce the reported, large-amplitude increases. However, it was found that the effect of two such regions, one located near the transmitter and one near the receiver, present simultaneously, could account for the observations. We reexamined this path with the newer model and found that the principal results did not change significantly. We refer the interested reader to Tolstoy [1983] for the details.

For the purpose of this study the more interesting data refer to the more recent multiple path observations at Palmer station which show that some paths are rarely disturbed while others have

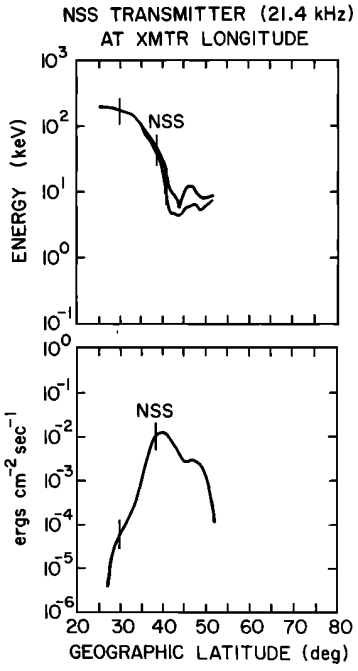

Fig. 3. Latitude profiles of electron energy and flux of transmitter-induced precipitation along the 77° W meridian through the NSS transmitter [from Inan, 1981]. The top panel gives the range of electron energies contributing to the energy flux in the bottom panel. Vertical lines indicate the latitudinal extent of the IE region adopted for the calculations in this paper.

particular disturbance patterns. Note that the calculations for all paths are normalized to a transmitter radiated power of 1 kW. When account is taken of the actual radiated powers (see Table 1), the predicted signal amplitudes are 20-30 dB higher than given in the figures and are within about 5 dB of the values observed for each path.

Most of the recent studies of Trimpi events [e.g., Carpenter and LaBelle, 1982; Leyser et al., 1984] involve measurements made at Palmer, located at the edge of the ice whose effects can be ignored until a few wavelengths beyond the boundary. The data include signals from NSS, NAA, NLK, and NPM. In general the NSS amplitude data show small to medium increases (a few decibels), the NAA signal is usually undisturbed but can show small increases, NLK shows occasional, small increases, and NPM shows many small negative changes.

4.1. NSS to Palmer

We began by examining the effects upon the NSS signal (at 21.4 kHz) of IE regions located near Palmer. The background signal is shown in Figure 4, and we notice that under background conditions, Palmer (P) is located somewhat before a signal maximum, i.e., in a region showing rapid signal change. Thus, we expected and found the signal to be quite sensitive to disturbances near Palmer. Both amplitude increases and decreases of several decibels can be produced by IE regions near the station. In general, the proximity of the region to the station was found to have far more effect than its size.

We considered the effects of IE regions produced by small fluxes (10^{-3} to 10^{-7} erg cm^{-2} s^{-1}) of 50-, 100- and 150-keV electrons. Figure 5 shows the amplitude changes that result from the indicated electron energies and fluxes precipitated into a 50-km-long region whose center is 575 km from Palmer. It is evident that higher-energy electrons cause larger signal perturbations for a given flux (10^{-7} erg cm^{-2} s^{-1} for the case shown). Furthermore, at constant energy (150 keV in Figure 5), increasing the flux from 10^{-7} to 10^{-5} also results in larger effects upon the signal. For a region located ~ 400 km from Palmer (a great circle distance of 11.2 Mm from NSS) the maximum amplitude increase was 2.1 dB for the 10^{-7} erg cm^{-2} s^{-1} flux and 5.7 dB for the 10^{-5} erg cm^{-2} s^{-1} flux.

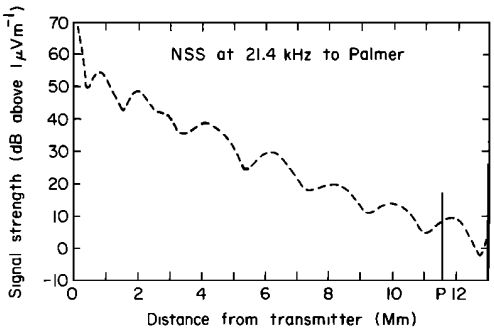

Fig. 4. Amplitude of the signal from NSS to Palmer (P) as a function of great circle distance from NSS. The dashed curve corresponds to an exponential background with $\beta = 0.47$ km^{-1}, $h' = 87$ km. In this and subsequent figures the signal amplitudes are normalized to a transmitted power of 1 kW. The actual amplitudes should be 20 - 30 dB higher depending on the transmitter (see Table 1 for the actual radiated powers).

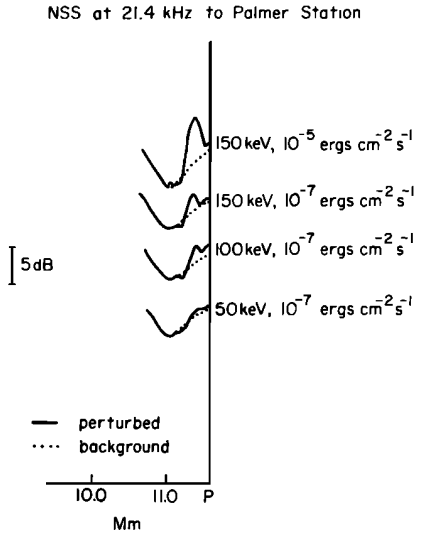

Fig. 5. Amplitude changes of the NSS signal near Palmer caused by IE regions of various electron precipitation energies and fluxes. The IE region in all cases is 50 km long and is centered 575 km from Palmer (P). Amplitude is measured in decibels above 1 μV m^{-1} as in Figure 4. The curves are offset for ease of comparison.

In general, we found that the amplitude change was proportional to the flux for very small fluxes ($\lesssim 10^{-5}$ erg cm^{-2} s^{-1}). However, a flux of 10^{-3} erg cm^{-2} s^{-1} at 150 keV produced perturbations only slightly larger than those for 10^{-5} erg cm^{-2} s^{-1} (not shown). This saturation effect appears to be a consequence of the fact that reflection of VLF energy at the nighttime ionospheric boundary of the waveguide is nearly complete below 87 km altitude where electron densities are in excess of 20 cm^{-3}. As shown in Figure 2 this density is achieved at 83 km for 10^{-7} erg cm^{-2} s^{-1} and at 75 km for 10^{-5} and 10^{-3} erg cm^{-2} s^{-1}. Note that a flux of 10^{-5} erg cm^{-2} s^{-1} at 150 keV is equivalent (if one assumes an exponential spectrum with E_0 ≈ 40 - 100 keV) to an energy deposition rate of ~ 3×10^{-3} erg cm^{-2} s^{-1} for E > 40 keV, which is of the same order as the measured electron fluxes in lightning-induced precipitation events [e.g., Voss et al., 1984; Goldberg et al., 1986].

In general, the saturation flux will depend on the energy spectrum of the precipitated electrons and the background electron density. Higher background densities below 87 km than those assumed here may apply over a portion of the paths near Palmer since there is evidence [e.g., Vampola and Gorney, 1983] that the average energy deposition into the atmosphere in the vicinity of Palmer from electrons of energies above a few tens of kilovolts may be of the order of 10^{-5} erg cm^{-2} s^{-1} or higher. Such precipitation would result in a lower background reference height h' over the affected portions of the paths. This would lead to different IE region parameters to produce the same effects. Nevertheless, a saturation flux

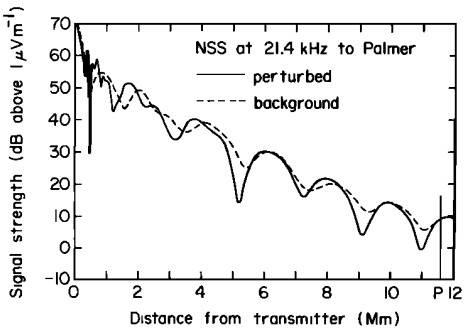

Fig. 6. Amplitude of the signal from NSS to Palmer (P) as a function of great circle distance from NSS. The dashed curve corresponds to an exponential background with $\beta = 0.47$ km^{-1}, h' = 87 km (same as in Figure 4). The solid curve shows the possible influence of transmitter-induced electron precipitation.

level would still occur whenever total electron densities of the order of 100 cm^{-3} are produced. For a given spectrum, the saturation levels in such cases would be higher.

We also note that while a saturation effect is observed when the flux is increased while keeping the size of the IE region constant, such a circumstance may not be representative of precipitation regions generated by whistlers. Indeed, both the spatial size and the spectral content of whistler-induced precipitations would be expected to be highly dependent on the flux level. Stronger lightning flashes would launch wave energy over a broader region within which precipitation might occur; similarly, higher fluxes would be expected to consist of particles having a wider range of energies [Chang and Inan, 1985], thus changing the density profile within the IE region.

Although the amplitude increases reported for Palmer can be explained by the IE regions examined, for completeness we also investigated the effects of predicted transmitter-induced electron precipitation. The signal perturbed by precipitation around NSS shows a more pronounced mode interference pattern than the background signal (see Figure 6); the effects on this perturbed signal of IE regions near Palmer were found to be larger than those on the background signal.

Thus, from the model predictions we conclude that (1) the size of the IE region (10 to 150 km) is relatively unimportant; (2) the higher-energy electrons have more effect on the VLF signal than the lower-energy electrons for a given flux; (3) increased flux results in increased signal perturbation (up to some maximum value); (4) very small flux levels (10^{-5} to 10^{-7} erg cm^{-2} s^{-1} depending on particle energy) can produce disturbances appropriate to those seen in the data; (5) the largest amplitude increases occurred for IE regions located ~ 400 km from Palmer; and (6) the sensitivity of the signal to IE regions near Palmer can be increased by the presence of transmitter-induced electron precipitation.

4.2. NAA to Palmer

The NAA transmitter is at a geomagnetic latitude (dip angle of 73.35 degrees) such that account should be taken of the change in h' with latitude for winter night conditions (see Table 2). Hence, we examined the NAA to Palmer signal under those conditions as well as under summer night conditions. Figure 7 shows that both of those signals (the solid and dotted curves) are almost identical beyond 1 Mm from NAA and become very flat beyond 8 Mm (the first TM (transverse magnetic) mode is strongly dominant). The effect of transmitter-induced electron precipitation (energies and fluxes for NAA can be found in the work by Inan et al. [1984]), if present, is to reduce the signal level, but retain almost identical character beyond 4 Mm to that of the undisturbed signals (see the dashed curve in Figure 7). The slight effect of this precipitation upon the signal is not surprising since at the high latitude of the NAA transmitter the precipitated electron energies are low (< 40 keV until 40 degrees north, or ~ 500 km south of NAA) while at the lower latitudes which are farther from NAA the predicted fluxes are too low to have much effect.

Consider next the effects on the signal of IE regions near Palmer. For regions at 350 km from Palmer resulting from the incidence of 150-keV electrons the signal usually shows amplitude increases with maximum values of 0.6 dB for a flux of 10^{-7} erg cm^{-2} s^{-1} and 3.2 dB for 10^{-5} erg cm^{-2} s^{-1}. This latter increase is much larger than has yet been reported. To summarize the NAA results, we find that: (1) the NAA signal is not significantly affected either by high-latitude winter effects or by transmitter-induced electron precipitation; (2) the NAA signal is less sensitive to perturbation than the NSS signal; and (3) the NAA signal will usually show increases for IE regions near Palmer.

4.3. NLK to Palmer

As a function of distance from NLK to Palmer this signal shows a strong mode interference pattern with Palmer located just after an amplitude maximum (see the dashed curve of Figure 8). The effect of transmitter-induced electron precipita-

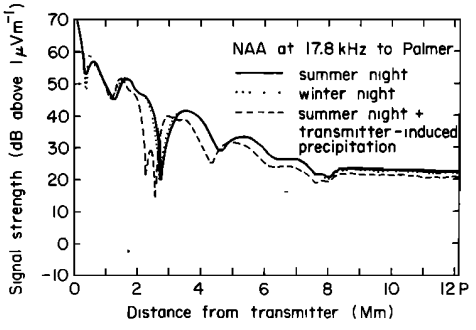

Fig. 7. Amplitude of the signal from NAA to Palmer (P) as a function of great circle distance from NAA. The solid curve corresponds to the Ferguson [1980] exponential background for summer night conditions with $\beta = 0.45$ km^{-1}, h' = 87 km. The dotted curve corresponds to winter night conditions with high-latitude effects near NAA, and the dashed curve to summer night plus the influence of transmitter-induced electron precipitation.

tion was also considered. The signal showed a stronger mode interference pattern overall (see the solid curve of Figure 8) but similar behavior near Palmer. For both conditions, IE regions placed within 500 km of Palmer (at great circle distances of 13.0 to 13.5 Mm from NLK) are interacting with a slowly changing signal. Hence, we expected and found the signal to be somewhat insensitive to IE regions near Palmer. We can summarize the results for this path as follows: (1) IE regions generally produce small increases in the NLK signal amplitude when the region is located farther than 150 km from Palmer; small decreases can also occur but are probably less frequent; and (2) transmitter-induced electron precipitation does not significantly change the NLK signal in the neighborhood of Palmer.

4.4. NPM to Palmer

The great circle path from NPM to Palmer is an all-seawater path showing an essentially flat amplitude plot near Palmer (Figure 9). Hence, we expected and found the NPM signal to be relatively insensitive to IE regions near Palmer. However, small amplitude decreases could be produced. Transmitter-induced electron precipitation would be expected to be mostly negligible, owing to the very low geomagnetic latitude of the NPM transmitter [Inan et al., 1982].

4.5. Summary of Results Specific to Palmer

The effects of IE regions produced by 10^{-7} erg cm^{-2} s^{-1} of 150 keV electrons on the amplitude of signals from NSS, NAA, NLK, and NPM received at Palmer are summarized in Figure 10. Approximate magnitudes and signs (increasing or decreasing) of individual amplitude changes at Palmer are shown as a function of the distance of the IE regions (50 km long in all cases) from the receiver. In addition, these results together with calculations of phase changes are shown in Table 3. Note that phase retardations as well as phase advances are predicted by this model. Such behavior has been observed in recent data and is difficult to predict with single mode models [Inan et al., 1985]. In the examples of Figure 10 and Table 3, phase changes of up to ~ 3 μs are obtained, consistent

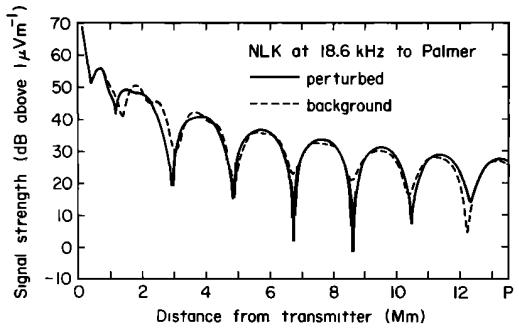

Fig. 8. Amplitude of the signal from NLK to Palmer (P) as a function of great circle distance from NLK. The dashed curve corresponds to an exponential background with $\beta = 0.45$ km^{-1}, $h' = 87$ km. The solid curve shows the influence of transmitter-induced electron precipitation.

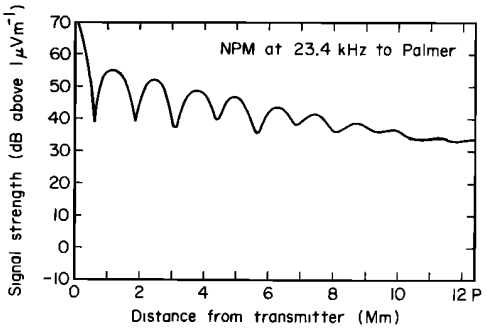

Fig. 9. Amplitude of the signal from NPM to Palmer (P) as a function of great circle distance from NPM for an exponential background with $\beta = 0.49$ km^{-1}, $h' = 87$ km.

with values observed on some of these paths [Inan et al., 1985].

In general, we find that the NSS signal is the most sensitive to perturbation of those signals examined. Disturbances of over 2 dB can be produced by small IE regions of high-energy electrons precipitating in very small fluxes near Palmer. Larger effects are predicted if the NSS signal is also disturbed by transmitter-induced electron precipitation. IE regions near Palmer produce relatively small effects upon the NAA, NLK, and NPM signals. With respect to the size of events on NSS and the relative sizes of amplitude changes on the several observed signals, these results are consistent with observed data.

5. Summary and Conclusions

For this study we used a waveguide mode theoretic propagation model to examine the effect of electron ionization enhancement (IE) regions on a variety of VLF signals. The model included both mode conversion and changing ground conductivity along the propagation path. Currently accepted background ionospheric profiles for electron density as well as profiles predicted to result from transmitter-induced electron precipitation were incorporated. Our study examined the NSS signal received at Eights and signals from several transmitters (NSS, NAA, NLK, NPM) received at Palmer.

Propagation model predictions of signal amplitude show that each transmitter to receiver path has a unique character, and thus each path reacts differently to the same IE regions. The most important factors affecting those paths under uniform background conditions are the transmitter frequency, geographic location, the electron density profile, and the ground conductivities encountered. As a result of the interplay of these parameters, it is necessary to perform full model calculations for each path in order to deduce the effect of an IE region.

The model computations applied to the multiple path observations at Palmer are able to reproduce a number of the general features of the data. We conclude that the NSS signal is most sensitive to IE regions near the receiver; that amplitude increases predominate; that the largest amplitude increases occur for IE regions located ~ 400 km from Palmer; and that signal sensitivity increases with the presence of transmitter-induced electron

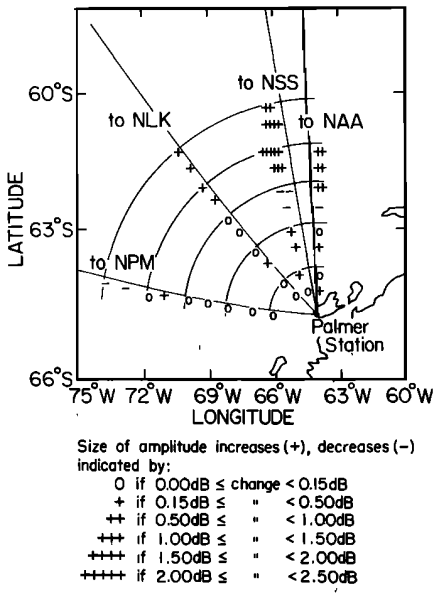

Fig. 10. The amplitude effects of IE regions on NSS, NAA, NLK, and NPM signals at Palmer. The plus and minus signs indicate the size and sense of amplitude changes observed at Palmer for an IE region located at the sign. A region 50 km in length resulting from 150-keV electrons with a flux of 10^{-7} erg cm^{-2} s^{-1} is assumed. Distance is given by the circular segments at intervals of 100 km from Palmer.

precipitation. For the NAA signal at Palmer we find that the signal changes little in the presence of transmitter-induced electron precipitation or as the result of possible high-latitude winter effects near the transmitter. The NAA signal usually shows amplitude increases for IE regions near Palmer but is much less easily perturbed by small fluxes than is NSS. The NLK signal shows small increases for IE regions near Palmer and is not significantly affected by the presence of transmitter-induced electron precipitation. NPM shows small decreases for IE regions located at least 200 km from Palmer.

In general, for long-path VLF signals recorded at Antarctic receivers we conclude that: (1) the size of the IE region is less important than its distance from the receiver; (2) for a given flux level, higher-energy electrons have larger effects on the signals than do lower-energy electrons; and (3) larger fluxes result in larger amplitude change.

The model calculations, performed for a monoenergetic spectrum of 150-keV electrons and for a nighttime ionospheric VLF reflecting height h' of 87 km, predict a saturation of the effect in (3) for fluxes larger than ~ 10^{-5} erg cm^{-2} s^{-1}, assuming that the size of the IE region is independent of flux level. This latter condition, however, may not be representative of whistler-induced precipitation. The above flux is equivalent to ~ 3×10^{-3} erg cm^{-2} s^{-1} for E > 40 keV assuming exponential electron spectra with e-folding energies of 40 - 100 keV. The measurements of Voss et al. [1984] and Goldberg et al. [1986] and the calculations by Chang and Inan [1985] indicate that electron fluxes of the order of 10^{-3} erg cm^{-2} s^{-1} are involved in Trimpi events. If h' near Palmer were lower owing, for example, to the presence of quiet time energetic electron precipitation, then higher whistler-induced fluxes (for a given spectrum) would be required before this saturation effect would occur in Trimpi events. (Note that a saturation effect on nighttime VLF phase was pointed out previously by Potemra and Rosenberg [1973] in connection with events on the spatial and temporal scale of substorms.)

The model calculations support the hypothesis that whistlers can induce the precipitation of small localized fluxes of energetic electrons which subsequently perturb the nighttime VLF signals passing through those regions. Furthermore, predictions as to the effects of such regions on the VLF signals can be made including inferences about a region's approximate location, size, and particle characteristics (energy and flux level). Lastly, the calculations suggest that transmitter-induced electron precipitation, which is known to occur, may on occasion have important effects on nighttime VLF propagation, particularly as shown here for the NSS signal.

Further studies will be concerned with the application of the model to shorter paths and to

TABLE 3. Predicted Amplitude (ΔA) and Phase (Δt) Changes of VLF Signals Received at Palmer, Antarctica

Distance From	NSS		NAA		NLK		NPM	
Palmer, km	ΔA, dB	Δt, μs	ΔA, dB	Δt, μs	ΔA, dB	Δt, μs	ΔA, dB	Δt, μs
50	0.12	1.97	0.29	-1.27	-0.04	0.10	--	--
100	0.18	0.27	-0.02	0.20	-0.08	-0.06	0.04	0.04
150	0.22	1.57	0.21	0.11	0.16	-0.09	-0.05	0.10
200	0.42	2.22	0.00	-2.81	0.10	1.00	-0.06	-0.04
250	-0.25	1.21	-0.42	0.96	0.00	0.26	0.07	-0.11
300	-0.85	0.87	0.62	2.83	-0.05	0.00	-0.02	0.04
350	1.22	-1.59	0.64	-0.59	0.40	-0.27	0.24	0.50
400	2.08	0.61	0.95	-2.62	0.28	0.20	0.02	0.83
450	1.52	2.78	--	--	0.38	0.16	-0.27	0.79
500	0.63	2.89	--	--	0.39	0.91	-0.34	0.49

The location of the IE region (150-keV electrons, 10^{-7} erg cm^{-2} s^{-1}, 50 km length) is given in the first column; Δt positive corresponds to phase advance.

higher- and lower-frequency signals, and with the correlation of phase predictions with recently obtained phase data. Extension of the model to three-dimensional capability is also intended. Combining multiple path data with a model that can treat the spatial extent of the perturbed region in three dimensions offers the promise of being able to locate more precisely the IE region corresponding to a given Trimpi event.

Acknowledgments. The typescript was prepared by B. Casanova. This work was supported by the Division of Polar Programs of the National Science Foundation under grants DPP 8012941 and DPP 8217260 and by the Computer Science Center of the University of Maryland. The work at Stanford University was supported under grants DPP 8217820 and DPP 8317092.

The Editor thanks W. L. Imhof and H. J. Strangeways for their assistance in evaluating this paper.

References

Budden, K. G., Radio Waves in the Ionosphere, Cambridge University Press, New York, 1961.

Cain, J. C., S. J. Hendricks, R. A. Langel, and W. V. Hudson, A proposed model for the international geomagnetic reference field - 1965, J. Geomagn. and Geoelectr., 19, 335, 1967.

Carpenter, D. L., and J. W. LaBelle, A study of whistlers correlated with bursts of electron precipitation near L = 2, J. Geophys. Res., 87, 4427, 1982.

Carpenter, D. L., U. S. Inan, M. L. Trimpi, R. A. Helliwell, and J. P. Katsufrakis, Perturbations of subionospheric LF and MF signals due to whistler-induced electron precipitation bursts, J. Geophys. Res., 89, 9857, 1984.

Carpenter, D. L., U. S. Inan, E. W. Paschal, and A. J. Smith, A new VLF method for studying burst precipitation near the plasmapause, J. Geophys. Res., 90, 4383, 1985.

Chang, H. C., and U. S. Inan, A theoretical model study of observed correlations between whistler mode waves and energetic electron precipitation events in the magnetosphere, J. Geophys. Res., 88, 10,053, 1983.

Chang, H. C., and U. S. Inan, Lightning-induced electron precipitation from the magnetosphere, J. Geophys. Res., 90, 1531, 1985.

Dingle, B., Burst precipitation of energetic electrons from the magnetosphere, Ph.D. thesis, Stanford Univ., Stanford, Calif., 1977.

Dingle, B., and D. L. Carpenter, Electron precipitation induced by VLF noise bursts at the plasmapause and detected at conjugate ground stations, J. Geophys. Res., 86, 4597, 1981.

Doolittle, J. H., and D. L. Carpenter, Photometric evidence of electron precipitation induced by first hop whistlers, Geophys. Res. Lett., 10, 611, 1983.

Ferguson, J. A., Ionospheric profiles for predicting nighttime VLF/LF propagation, Tech. Rep. 530, Nav. Ocean Syst. Command, San Diego, Calif., 1980.

Foster, J. C., and T. J. Rosenberg, Electron precipitation and VLF emissions associated with cyclotron resonance interactions near the plasmapause, J. Geophys. Res., 81, 2183, 1976.

Goldberg, R. A., S. A. Curtis, J. R. Barcus, C. L. Siefring, and M. C. Kelley, Controlled stimulation of magnetospheric electrons by radio waves: Experimental model for lightning effects, Science, 219, 1324, 1983.

Goldberg, R. A., J. R. Barcus, L. C. Hale, and S. A. Curtis, Direct observation of magnetospheric electron precipitation stimulated by lightning, J. Atmos. Terr. Phys., 48, 293, 1986.

Helliwell, R. A., J. P. Katsufrakis, and M. L. Trimpi, Whistler-induced amplitude perturbation in VLF propagation, J. Geophys. Res., 78, 4679, 1973.

Helliwell, R. A., S. B. Mende, J. H. Doolittle, W. C. Armstrong, and D. L. Carpenter, Correlations between λ4278 optical emissions and VLF wave events observed at L ~ 4 in the Antarctic, J. Geophys. Res., 85, 3376, 1980.

Imhof, W. L., R. R. Anderson, J. B. Reagan, and E. E. Gaines, The significance of VLF transmitters in the precipitation of inner belt electrons, J. Geophys. Res., 86, 11,225, 1981.

Imhof, W. L., J. B. Reagan, H. D. Voss, E. E. Gaines, D. W. Datlowe, J. Mobilia, R. A. Helliwell, U. S. Inan, and J. Katsufrakis, The modulated precipitation of radiation belt electrons by controlled signals from VLF transmitters, Geophys. Res. Lett., 10, 615,1983.

Inan, U. S., A preliminary study of particle precipitation induced by VLF transmitter signals, Tech. Rep. E477-1, Stanford Electron. Lab., Stanford Univ., Stanford, Calif., 1981.

Inan, U. S., T. F. Bell, and H. C. Chang, Particle precipitation induced by short-duration VLF waves in the magnetosphere, J. Geophys. Res., 87, 6243, 1982.

Inan, U. S., H. C. Chang, and R. A. Helliwell, Electron precipitation zones around major ground-based VLF signal sources, J. Geophys. Res., 89, 2891, 1984.

Inan, U. S., D. L. Carpenter, R. A. Helliwell, and J. P. Katsufrakis, Subionospheric VLF/LF phase perturbations produced by lightning-whistler induced particle precipitation, J. Geophys. Res., 90, 7457, 1985.

Kintner, P. M., and J. LaBelle, Very short path length Trimpi observations, Eos Trans. AGU, 65, 1059, 1984.

Leyser, T. B., U. S. Inan, D. L. Carpenter, and M. L. Trimpi, Diurnal variation of burst precipitation effects on subionospheric VLF/LF signal propagation near L = 2, J. Geophys. Res., 89, 9139, 1984.

Lohrey, B., and A. B. Kaiser, Whistler-induced anomalies in VLF propagation, J. Geophys. Res., 84, 5122, 1979.

Morfitt, D. G., and C. H. Shellman, MODESRCH, an improved computer program for obtaining ELF/VLF/LF mode constants in an earth-ionosphere waveguide, Interim Rep. 77T, Nav. Electron. Lab. Cent., San Diego, Calif., Oct. 1, 1976.

Pappert, R. A., and F. P. Snyder, Some results of a mode-conversion program for VLF, Radio Sci., 7, 913, 1972.

Potemra, T. A., and T. J. Rosenberg, VLF propagation disturbances and electron precipitation at mid-latitudes, J. Geophys. Res., 78, 1572, 1973.

Rees, M. H., Auroral ionization and excitation by incident energetic electrons, Planet. Space Sci., 11, 1209, 1963.

Rosenberg, T. J., R. A. Helliwell, and J. P. Katsufrakis, Electron precipitation associated with discrete very-low-frequency emissions, J. Geophys. Res., 76, 8445, 1971.

Rosenberg, T. J., J. C. Siren, D. L. Matthews, K. Marthinsen, J. A. Holtet, A. Egeland, D. L. Carpenter, and R. A. Helliwell, Conjugacy of electron microbursts and VLF chorus, J. Geophys. Res., 86, 5819, 1981.

Rycroft, M. J., Enhanced energetic electron intensities at 100 km altitude and a whistler propagating through the plasmasphere, Planet. Space Sci., 21, 239, 1973.

Thomas, L., The effects of ions on the propagation of ELF and VLF waves in the lower ionosphere, J. Atmos. Terr. Phys., 31, 991, 1969.

Tolstoy, A., The influence of localized precipitation-induced D-region ionization enhancements on subionospheric VLF propagation, Tech. Rep. BN-1011, Univ. of Maryland, College Park, 1983.

Tolstoy, A., and T. J. Rosenberg, A quasi three-dimensional propagation model for subionospherically propagating VLF radio waves, Radio Sci., 20, 535, 1985.

Tolstoy, A., T. J. Rosenberg, and D. L. Carpenter, The influence of localized precipitation-induced D-region ionization enhancements on subionospheric VLF propagation, Geophys. Res. Lett., 9, 563, 1982.

Vampola, A. L., and D. J. Gorney, Electron energy deposition in the middle atmosphere, J. Geophys. Res., 88, 6267, 1983.

Voss, H. D., W. L. Imhof, M. Walt, J. Mobilia, E. E. Gaines, J. B. Reagan, U. S. Inan, R. A. Helliwell, D. L. Carpenter, J. P. Katsufrakis, and H. C. Chang, Lightning-induced electron precipitation, Nature, 312, 740, 1984.

Wait, J. R., Electromagnetic Waves in Stratified Media, 2nd ed., Pergamon, New York, 1970.

Wait, J. R., and K. P. Spies, Characteristics of the earth-ionosphere waveguide for VLF radio waves, Tech. Note 300, Natl. Bur. of Stand., Boulder, Colo., 1964.

D. L. Carpenter and U. S. Inan, Space, Telecommunications and Radioscience Laboratory, Stanford University, Stanford, CA 94305.

T. J. Rosenberg, Institute for Physical Science and Technology, University of Maryland, College Park, MD 20742.

A. Tolstoy, Naval Research Laboratory, Code 5120, Washington, DC 20375.

(Received March 26, 1986;
revised July 17, 1986;
accepted July 30, 1986.)